Mixed-phase wavelet estimation by iterative linear inversion of high-order statistics

2007 J. Geophys. Eng. 4 184

(http://iopscience.iop.org/1742-2140/4/2/007)

IOP Publishing Journal of Geophysics and Engineering
J. Geophys. Eng. **4** (2007) 184–193 doi:10.1088/1742-2132/4/2/007

Mixed-phase wavelet estimation by iterative linear inversion of high-order statistics

Xiaolin Lü and Yanghua Wang

Centre for Reservoir Geophysics, Department of Earth Science and Engineering, Imperial College, London SW7 2AZ, UK

E-mail: yanghua.wang@imperial.ac.uk

Received 30 November 2006
Accepted for publication 13 February 2007
Published 23 March 2007
Online at stacks.iop.org/JGE/4/184

Abstract
This is a review paper on the mixed-phase wavelet estimation using high-order statistics. We use an iterative linear inversion method as a primary thread, stringing together others including the maximum time-delayed moment (MTM) method and the normalized cumulant (NC) method. Both MTM and NC methods are not stable, because they make use of only single high-order-statistics slices. As for the iterative linear inversion method, it is stable but needs a good initial model. Therefore, we adopt a hybrid strategy that uses the MTM or NC method to generate an initial estimate of the wavelet for the iterative linear inversion method. The real seismic data test has shown that all inversions with different initial models converge to the same result within allowable accuracy. Therefore, the iterative linear inversion method is applicable to real multi-channel seismic data for wavelet estimation.

Keywords: mixed-phase wavelet, high-order statistics, fourth-order cumulant, third-order moment, inversion

(Some figures in this article are in colour only in the electronic version)

1. Introduction

Seismic wavelet estimation is an important issue in seismic data processing and inversion. During the course of wave propagation, the wavelet excited by a seismic source that has a fixed amplitude and phase spectra will alter both in amplitude and phase, and the resultant wavelet is usually with the mixed phase, varying in time and space. In seismic inversion, only after the accurate extraction of the mixed-phase wavelet can we have a reliable estimation of the reflectivity series.

For the mixed-phase wavelet estimation, the essential issue is how to accurately extract the phase information of the wavelet. High-order statistics can preserve the phase information of a system (Mendel 1991). Giannakis (1987) showed that the impulse response of a moving average system could be calculated just from the system's output cumulants, and then proposed a normalized cumulant (NC) method for wavelet estimation. Lazear (1993) presented a fourth-order cumulant (FOC) matching technique for mixed-phase wavelet estimation in which the wavelet is updated iteratively until its fourth-order statistics match those of the seismic data. This is a highly nonlinear optimization problem, for which Velis and Ulrych (1996) adopted a simulated annealing (SA) strategy for moment (windowed cumulant) matching. The SA-inversion method is reliable and accurate but, because of great time consumption, is suitable for generating only the single trace result. Sacchi and Ulrych (2000) used the cepstrum of the fourth-order cumulant to derive the minimum and maximum phase components of the wavelets. Lu (2005) proposed a maximum time-delayed moment (MTM) method to estimate the phase spectrum of the wavelet from its third-order moments without optimization or inversion. For the latter method, Velis and Sacchi (2006) discussed the reliability. Lu *et al* (2007) also tried to use the zero-lag slice of the fourth-order moment (FOM) for estimating seismic wavelets.

This is a review paper on mixed-phase wavelet estimation using high-order statistics. In this paper, we use an iterative linear inversion method for the moment matching as a primary thread, stringing together others mentioned above including the MTM method and NC method.

We will show that both MTM and NC methods are not stable, because both of them make use of only single high-order-statistics slices. Therefore, we use the MTM or NC method to generate an initial wavelet estimate for the iterative linear inversion. Given a sufficiently good initial estimate, we perform iteratively the linear inversion of moment matching. This method includes stabilization in the matrix inversion, and is robust for the wavelet estimation of real seismic data with wide spatial coverage. Then, an optimal wavelet can be selected from the multi-channel wavelet estimates.

2. High-order statistics of seismic traces and wavelets

Moments and cumulants are high-order covariance functions which are very useful for describing both deterministic and stochastic signals. For the sake of completeness, this section summarizes the basics of high-order statistics and their applicability for seismic signal analysis.

The kth-order moment function of a real stationary discrete-time signal, $x(t)$, is defined as (Mendel 1991)

$$m_k^x(\tau_1, \tau_2, \ldots, \tau_{k-1}) = E\{x(t)x(t+\tau_1)\cdots x(t+\tau_{k-1})\}, \quad (1)$$

where $E\{\cdot\}$ denotes statistical expectation. Cumulants may be expressed through moments. The kth-order cumulant function of a real stationary process is given by (Velis and Ulrych 1996)

$$c_k^x(\tau_1, \tau_2, \ldots, \tau_{k-1}) = E\{x(t)x(t+\tau_1)\cdots x(t+\tau_{k-1})\} - E\{g(t)g(t+\tau_1)\cdots g(t+\tau_{k-1})\}, \quad (2)$$

where $g(t)$ is an equivalent Gaussian process that has the same second-order statistics as $x(t)$. Cumulants not only display the amount of higher order correlation, but also provide a measure of the distance of the random process from Gaussianity. Obviously, for the third or high order, if $x(t)$ is Gaussian, $c_k^x(\tau_1, \tau_2, \ldots, \tau_{k-1}) = 0$. The second-, third- and fourth-order cumulants of a zero mean $x(t)$ are given explicitly as (Mendel 1991)

$$c_2^x(\tau) = E\{x(t)x(t+\tau)\}, \quad (3)$$

$$c_3^x(\tau_1, \tau_2) = E\{x(t)x(t+\tau_1)x(t+\tau_2)\}, \quad (4)$$

$$c_4^x(\tau_1, \tau_2, \tau_3) = E\{x(t)x(t+\tau_1)x(t+\tau_2)x(t+\tau_3)\} - c_2^x(\tau_1)c_2^x(\tau_2-\tau_3) - c_2^x(\tau_2)c_2^x(\tau_3-\tau_1) - c_2^x(\tau_3)c_2^x(\tau_1-\tau_2). \quad (5)$$

Consider a convolutional seismic model

$$x(t) = w(t) * r(t) + n(t), \quad (6)$$

where $w(t)$ is a seismic wavelet, $r(t)$ is a reflectivity function, $*$ is a convolutional operator and $n(t)$ is a term for noise. The Bartlett–Brillinger–Rosenblatt equation (Mendel 1991) denotes a relationship among the high-order statistics for the convolutional model. That is,

$$c_k^x(\tau_1, \ldots, \tau_{k-1}) = c_k^r(\tau_1, \ldots, \tau_{k-1}) * m_k^w(\tau_1, \ldots, \tau_{k-1}) + c_k^n(\tau_1, \ldots, \tau_{k-1}), \quad (7)$$

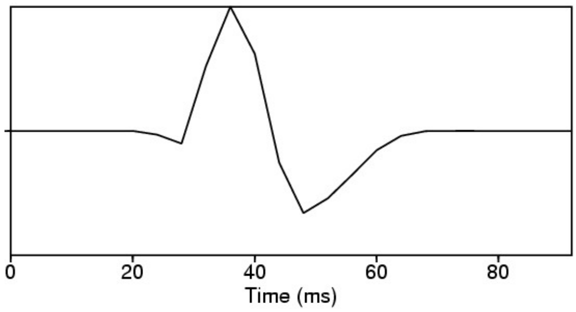

(*a*)

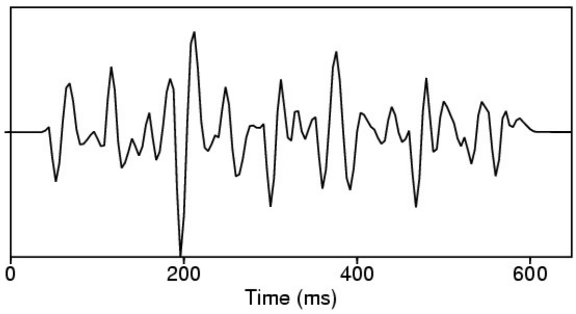

(*b*)

Figure 1. (*a*) A zero-mean synthetic wavelet, and (*b*) a synthetic seismic trace obtained by convolving the wavelet with a sparse reflectivity series.

where $c_k^r(\tau_1, \ldots, \tau_{k-1})$ and $c_k^n(\tau_1, \ldots, \tau_{k-1})$ are the kth-order cumulant of the reflectivity sequence and the noise, respectively, and $m_k^w(\tau_1, \ldots, \tau_{k-1})$ is the kth-order moment of the wavelet. Assuming that $r(t)$ is independent, identically distributed (IID) and non-Gaussian, the cumulant of $r(t)$ becomes

$$c_k^r(\tau_1, \ldots, \tau_{k-1}) = \begin{cases} \gamma_k^r, & \text{for} \quad \tau_1 = \cdots = \tau_{k-1} = 0, \\ 0, & \text{otherwise}, \end{cases} \quad (8)$$

where $\gamma_k^r = c_k^r(0, \ldots, 0)$ is the kurtosis of the reflectivity. Meanwhile, if the additive noise $n(t)$ is assumed to be Gaussian (but need not be white), which means its third and higher order cumulants vanish, equation (7) will be simplified to

$$c_k^x(\tau_1, \ldots, \tau_{k-1}) = \gamma_k^r m_k^w(\tau_1, \ldots, \tau_{k-1}). \quad (9)$$

This equation states that the kth-order ($k > 2$) cumulants of the seismic data differ from the kth-order moments of the seismic wavelet only by a scalar. Therefore, it has been the starting point for most of the mixed-phase wavelet estimation methods based on high-order statistics (Lazear 1993, Velis and Ulrych 1996, and references therein).

In practice, however, neither the cumulant of the noise is zero nor is the cumulant of the reflectivity series a multidimensional spike at zero lag. Figure 1 gives a zero-mean wavelet and a synthetic seismic trace. Figures 2(*a*) and (*b*) show a view of the fourth-order moment slice (at $\tau_3 = 0$) of the wavelet and the fourth-order cumulant slice (at $\tau_3 = 0$) of the synthetic trace, and they do not differ only by a scalar at all.

To approximate the wavelet moment by using the seismic trace cumulant, one could apply a 3D smoothing-tapering

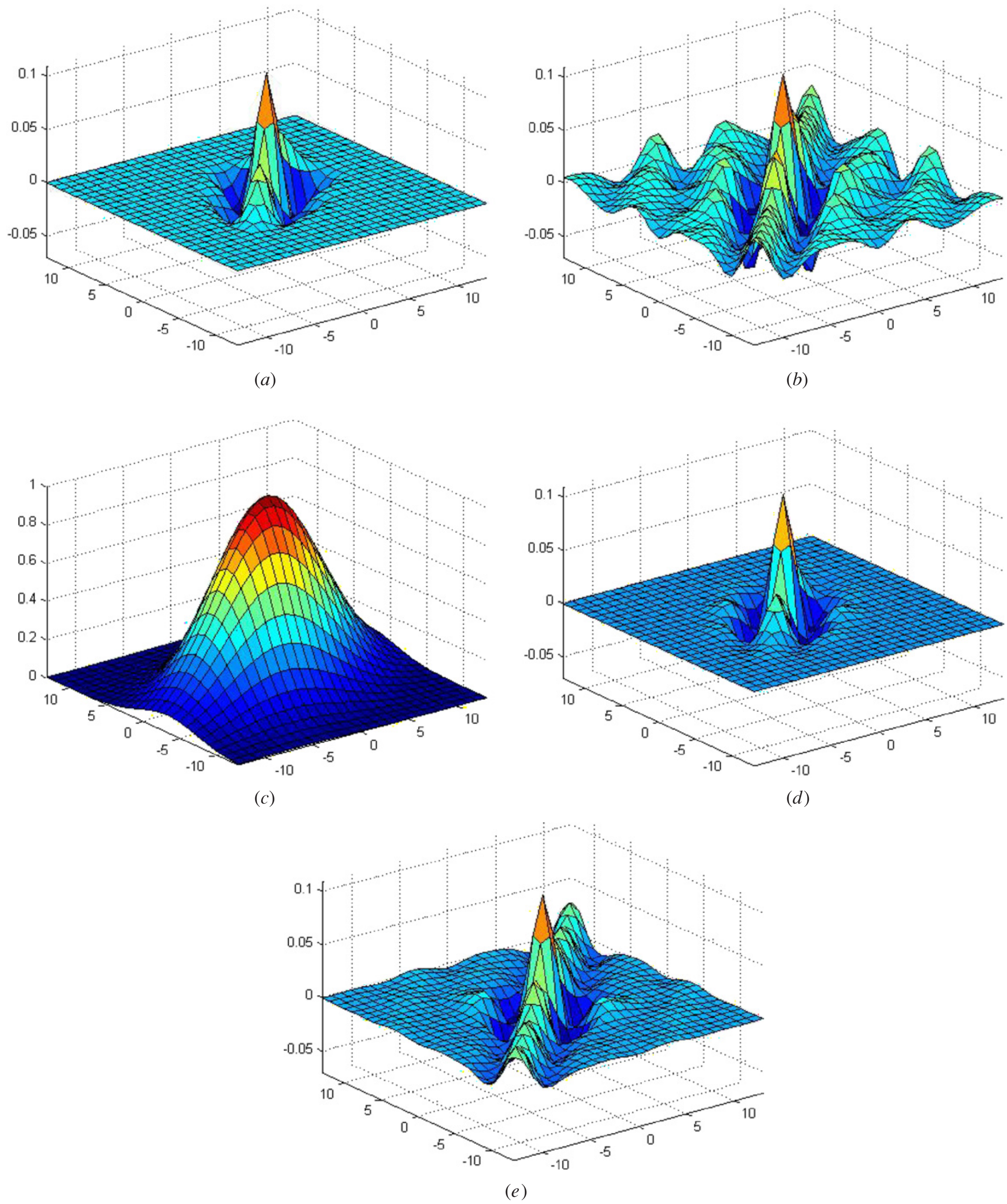

Figure 2. (*a*) A FOM slice of the wavelet in figure 1(*a*). (*b*) A FOC slice of the synthetic trace shown in figure 1(*b*). (*c*) A slice of the Parzen window. (*d*) An approximate FOM slice of the wavelet by windowing the FOC of the seismic trace. (*e*) A FOC slice of a very long seismic trace.

window to the seismic trace cumulant (Velis and Ulrych 1996). Equation (9) may be rewritten as

$$m_4^w(\tau_1, \tau_2, \tau_3) = \frac{1}{\gamma_4^r} a(\tau_1, \tau_2, \tau_3) c_4^x(\tau_1, \tau_2, \tau_3), \qquad (10)$$

where $a(\tau_1, \tau_2, \tau_3)$ is a 3D window function. The window function should have the following properties:

(1) $a(\tau_1, \tau_2, \tau_3) = a(-\tau_1, \tau_2 - \tau_1, \tau_3 - \tau_1) = a(\tau_1 - \tau_2, -\tau_2, \tau_3 - \tau_2) = a(\tau_1 - \tau_3, \tau_2 - \tau_3, -\tau_3)$ and any possible exchange of any pair of the three arguments (symmetry properties of the fourth-order statistics),

(2) $a(\tau_1, \tau_2, \tau_3) = 0$ for $|\tau_i| > L$ (where L defines the region involved in computation),

(3) $a(0, 0, 0) = 1$ for the normalizing condition.

It is easy to build the multidimensional window by using standard 1D windows. So we can write

$$a(\tau_1, \tau_2, \tau_3) = d(\tau_1)d(\tau_2)d(\tau_3)d(\tau_2 - \tau_1) \\ d(\tau_3 - \tau_2)d(\tau_3 - \tau_1), \qquad (11)$$

where $d(\tau) = d(-\tau)$, $d(\tau) = 0$ when $\tau > L$, $d(0) = 1$. Among many possible 1D windows (rectangular, triangular,

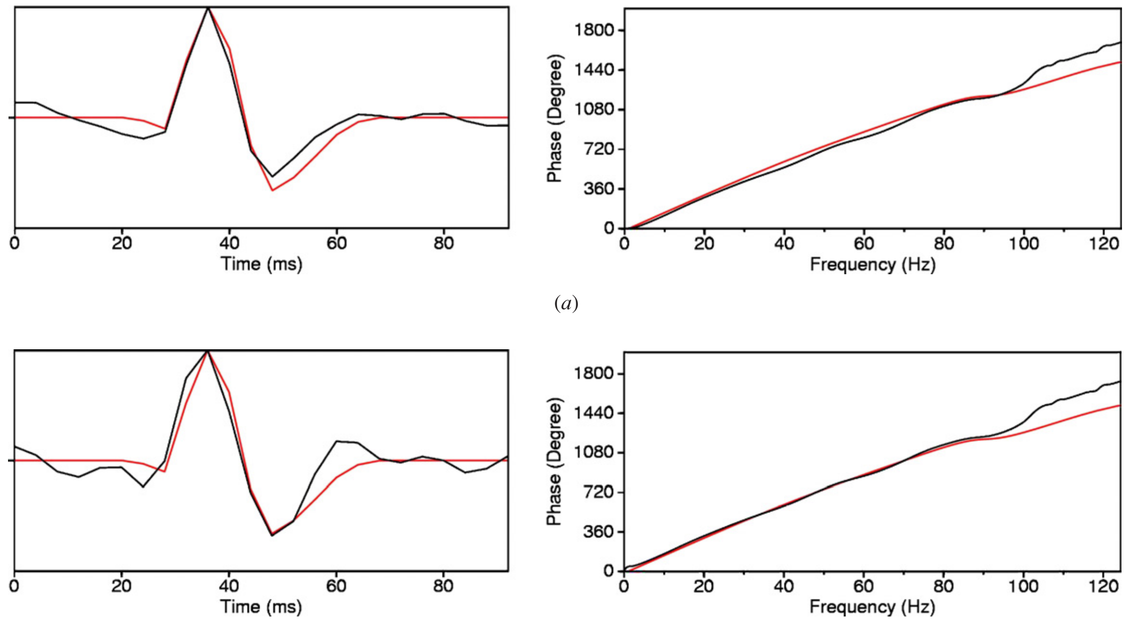

Figure 3. Wavelets estimated using the MTM method, and their phase spectra: (*a*) in MTM using the third-order moment directly; (*b*) in MTM using the third-order moment that is downgraded from the fourth-order moment. The red (grey) curve is the true wavelet and black curve is the estimated one.

Hamming, Gaussian, etc), Velis and Ulrych (1996) recommended a Parzen window defined by

$$d(\tau) = \begin{cases} 1 - 6(|\tau|/L)^2 + 6(|\tau|/L)^3, & |\tau| \leqslant L/2, \\ 2(1 - |\tau|/L)^3, & L/2 \leqslant |\tau| \leqslant L, \\ 0, & |\tau| > L. \end{cases} \tag{12}$$

Figure 2(*c*) shows a slice of the 3D Parzen window. Figure 2(*d*) shows the FOC slice ($\tau_3 = 0$) of the synthetic trace after applying the 3D Parzen window. Figure 2(*d*) is similar to figure 2(*a*), the FOM slice ($\tau_3 = 0$) of the zero-mean wavelet.

The estimated wavelet moment (figure 2(*d*)) is a distorted version of the true wavelet moment (figure 2(*a*)), because of the limited number of data in the seismic trace. Figure 2(*e*) is the FOC slice (at $\tau_3 = 0$) of a very long seismic trace (10 000 samples). The longer the seismic trace, the more accurate the wavelet FOM estimation we could have.

3. Two wavelet estimation methods

The main melody of this paper is the iterative linear inversion scheme for the wavelet estimation from real seismic data. For generating an initial estimate for the iterative inversion, we use two mixed-phase wavelet estimation methods overviewed in this section.

3.1. Maximum time-delayed moment method

Wavelet estimation may be divided into two stages: amplitude spectrum estimation and phase spectrum estimation. For amplitude spectrum estimation, we approximate the autocorrelation of the wavelet by windowing the autocorrelation of the seismic trace, which is also the second-order moment of the seismic data:

$$m_2^w(\tau) = d(\tau) m_2^x(\tau). \tag{13}$$

We obtain the amplitude spectrum of the expected wavelet $w(t)$ from the Fourier transform of $m_2^w(\tau)$.

For the phase spectrum estimation, the MTM method consists of the following main calculation steps: $m_3^w(\tau_1, \tau_2)$, $\tilde{r}(t) = m_3^r(t, D_{\max})$, and then for the phase spectrum of wavelet.

The third-order moments of the wavelet, $m_3^w(\tau_1, \tau_2)$, may be obtained by downgrading the fourth-order moments with a scale factor (Giannakis and Delopoulos 1995):

$$m_3^w(\tau_1, \tau_2) = \frac{1}{\alpha} \sum_{\tau_3} m_4^w(\tau_1, \tau_2, \tau_3), \tag{14}$$

where $\alpha = \sum_t w(t)$. Although the scalar α cannot be computed during the downgrade process from the fourth-order moments to the third-order moment of the wavelet, since $w(t)$ is just what we want to acquire finally, it is unnecessary to pay much attention to it because we only care about the relative values of the fourth-order moments during the stage of phase spectrum estimation.

Since the wavelet in our test is zero mean, which is usually the case in the real seismic wavelet, the seismic trace is also zero mean. Thus, the third-order moment of the seismic trace is identical to its third-order cumulant. According to equation (9), the third-order moment of the wavelet, $m_3^w(\tau_1, \tau_2)$, can also be obtained by

$$m_3^w(\tau_1, \tau_2) = a(\tau_1, \tau_2) c_3^x(\tau_1, \tau_2), \tag{15}$$

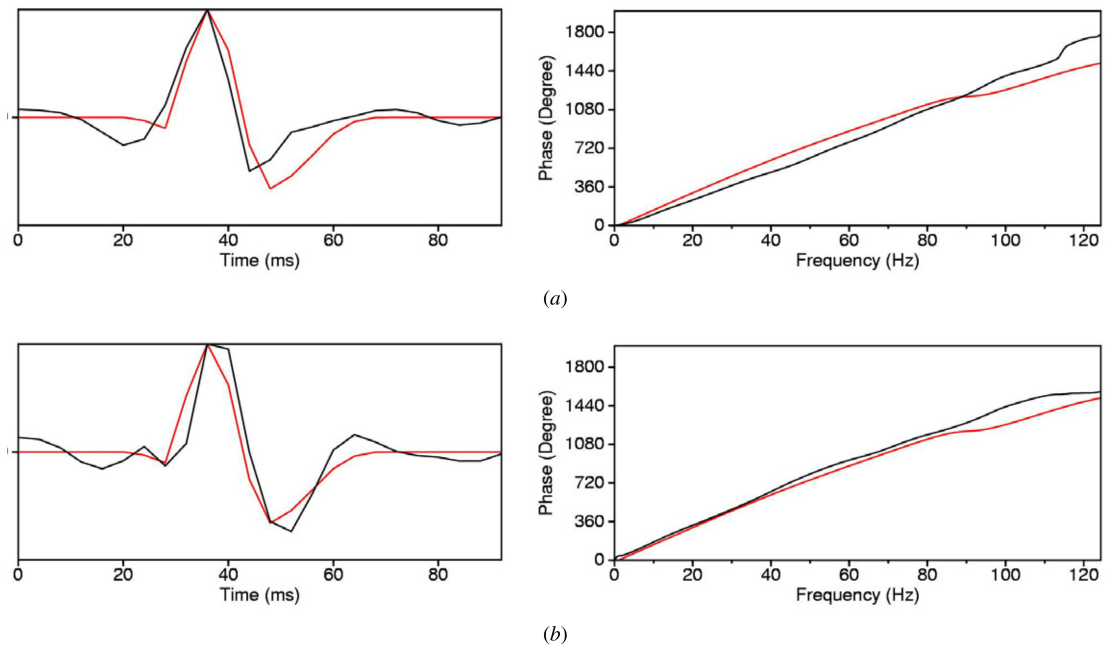

Figure 4. Wavelets estimated using the normalized cumulant method and the phase spectra of the wavelets: (*a*) using the third-order cumulant, and (*b*) using the fourth-order cumulant. The red (grey) curve is the true wavelet and the black one is the estimated wavelet.

where $c_3^x(\tau_1, \tau_2)$ is the third-order cumulant of the seismic trace and $a(\tau_1, \tau_2)$ is the 2D tapering window

$$a(\tau_1, \tau_2) = d(\tau_1)d(\tau_2)d(\tau_2 - \tau_1), \tag{16}$$

built using a 1D standard window $d(\tau)$. However, when the reflectivity coefficients in the convolution model are symmetrically distributed, the origin value of the third-order moment calculated by equation (15) is close to zero. Therefore, the downgrading method (equation (14)) is more stable for the wavelet estimation that follows.

The convolutional seismic model (equation (6)) can be expressed in a form of third-order moments

$$m_3^x(\tau_1, \tau_2) = m_3^w(\tau_1, \tau_2) * m_3^r(\tau_1, \tau_2), \tag{17}$$

if the noise is assumed to be Gaussian distributed. Once the third-order moment of the wavelet and the third-order moment of the seismic trace are obtained, the third-order moment of the reflectivity series can be derived by a division in the 2D frequency domain,

$$M_3^r(\omega_1, \omega_2) = M_3^x(\omega_1, \omega_2) \big/ M_3^w(\omega_1, \omega_2). \tag{18}$$

The inverse Fourier transformation of $M_3^r(\omega_1, \omega_2)$ produces $m_3^r(\tau_1, \tau_2)$, the third-order moment of the reflectivity series.

As summarized in the appendix, the maximum time-delayed slice is a scaled and time-shifted version of the reflectivity (Lu 2005):

$$\tilde{r}(t) = m_3^r(t, D_{\max}), \tag{19}$$

where $D_{\max}$ is the maximum time delay of the reflectivity $r(t)$, and is defined by

$$D_{\max} = d_N - d_1, \tag{20}$$

and d_i, for $i = 1, 2, \ldots, N$, is the location for the ith reflector in the sparse reflectivity series. The reflectivity may be approximated by

$$r(\omega) = \tilde{r}(\omega)\, e^{-i\omega d_1}/(a_1 a_N), \tag{21}$$

where a_i are the amplitude of the ith reflection. As $a_1 a_N$ is a scalar that is not responsible for the phase spectrum, we can estimate the wavelet phase spectrum in the frequency domain by

$$w(\omega) = \frac{x(\omega)}{\tilde{r}(\omega)}\, e^{i\omega d_1}. \tag{22}$$

Figure 3 displays the wavelet estimation results using the MTM method, and their phase spectra. In figure 3, (*a*) uses the third-order moment directly and (*b*) uses the third-order moment downgraded from the fourth-order moment. The relationship between the fourth-order moment and fourth-order cumulant was given by equation (10).

The key parameter in this method is $D_{\max}$, which must be identified from the original input seismic trace. It is subject to human error and is dependent on the data signal-to-noise ratio. Therefore, the MTM method is not stable for real data application.

3.2. Normalized cumulant method

Giannakis (1987) showed that the impulse response of a qth-order moving average (MA) system can be calculated just from the system's output cumulants. Therefore in the wavelet estimation problem, if the wavelet is a qth-order MA process and the reflectivity sequences satisfy non-Gaussian, which is IID, it can be proved that, for third-order cumulants,

$$w(t) = \frac{c_3^x(q, t)}{c_3^x(-q, -q)} = \frac{c_3^x(q, t)}{c_3^x(q, 0)}, \quad t = [0, q], \tag{23}$$

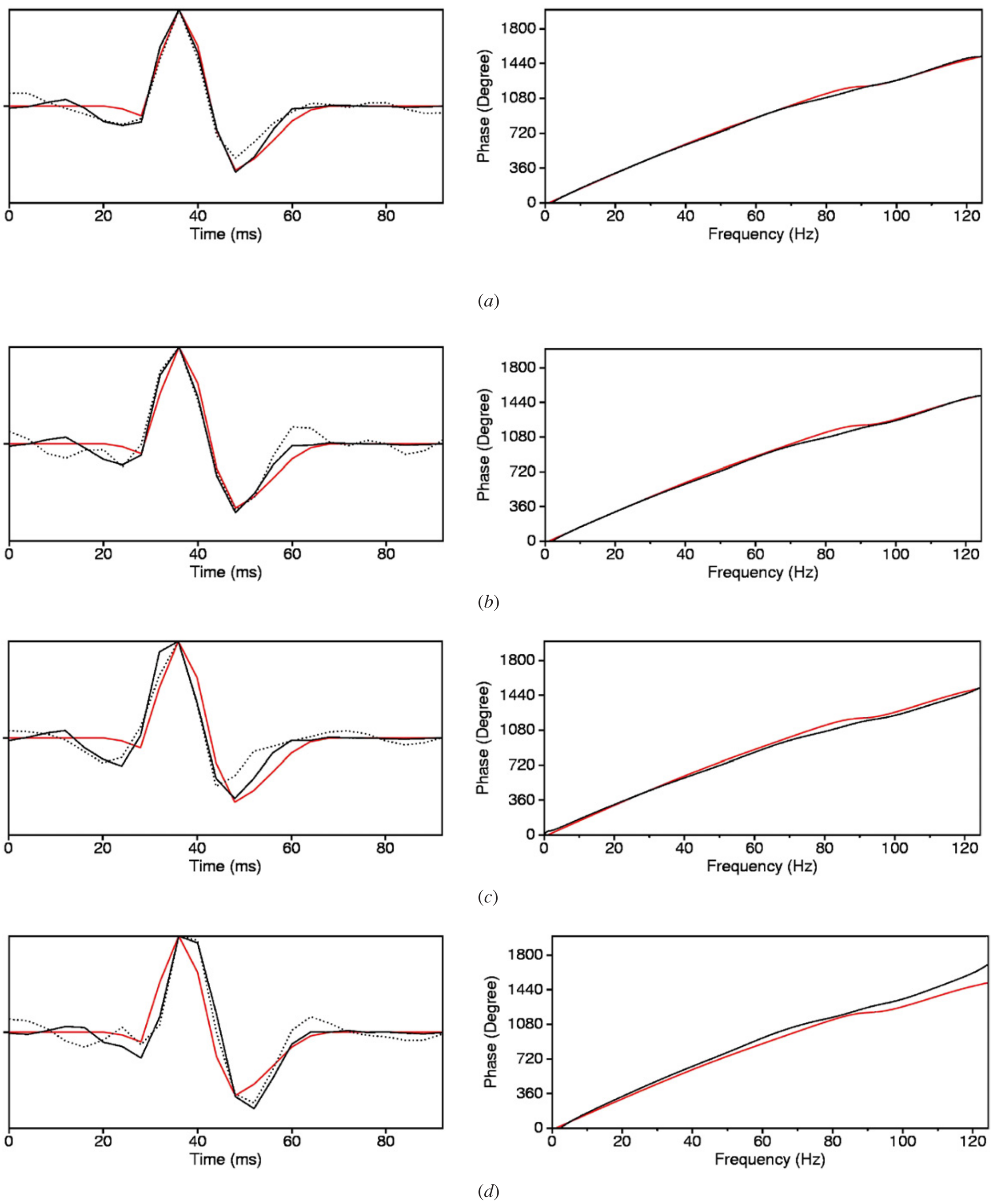

Figure 5. Wavelets estimated by using an iterative linear inversion method, and the phase spectra of wavelets: (*a*) the initial model generated from the third-order MTM and the linear inversion result; (*b*) the initial model generated from the fourth-order MTM and the linear inversion result; (*c*) the initial model generated from the third-order normalized cumulant method and the linear inversion result; (*d*) the initial model generated from the fourth-order normalized cumulant method and the linear inversion result. Each initial model (dotted curve) and inversion result (solid black curve) are compared to the true wavelet (red/grey curve).

and similarly, for fourth-order cumulants,

$$w(t) = \frac{c_4^x(q,0,t)}{c_4^x(-q,-q,-q)} = \frac{c_4^x(q,0,t)}{c_4^x(q,0,0)}, \quad t = [0,q]. \tag{24}$$

We refer to these two equations as the normalized cumulant method for wavelet estimation.

In most real seismic process cases, the wavelet is seldom a MA process, so we can only get a rough estimation of the mixed-phase wavelet. Figure 4 depicts the example results, both wavelets and phase spectra. In each wavelet, only the phase information from the normalized cumulant method is used. The amplitude spectrum is obtained from the windowed autocorrelation of the seismic trace, which is the same as in the previous MTM method.

The key parameter in the NC method is the q value. We set it to be the length of the expected wavelet, with an assumption that $c_3^x(\tau,t) \approx 0$ for every $\tau > q$ (Giannakis 1987). However,

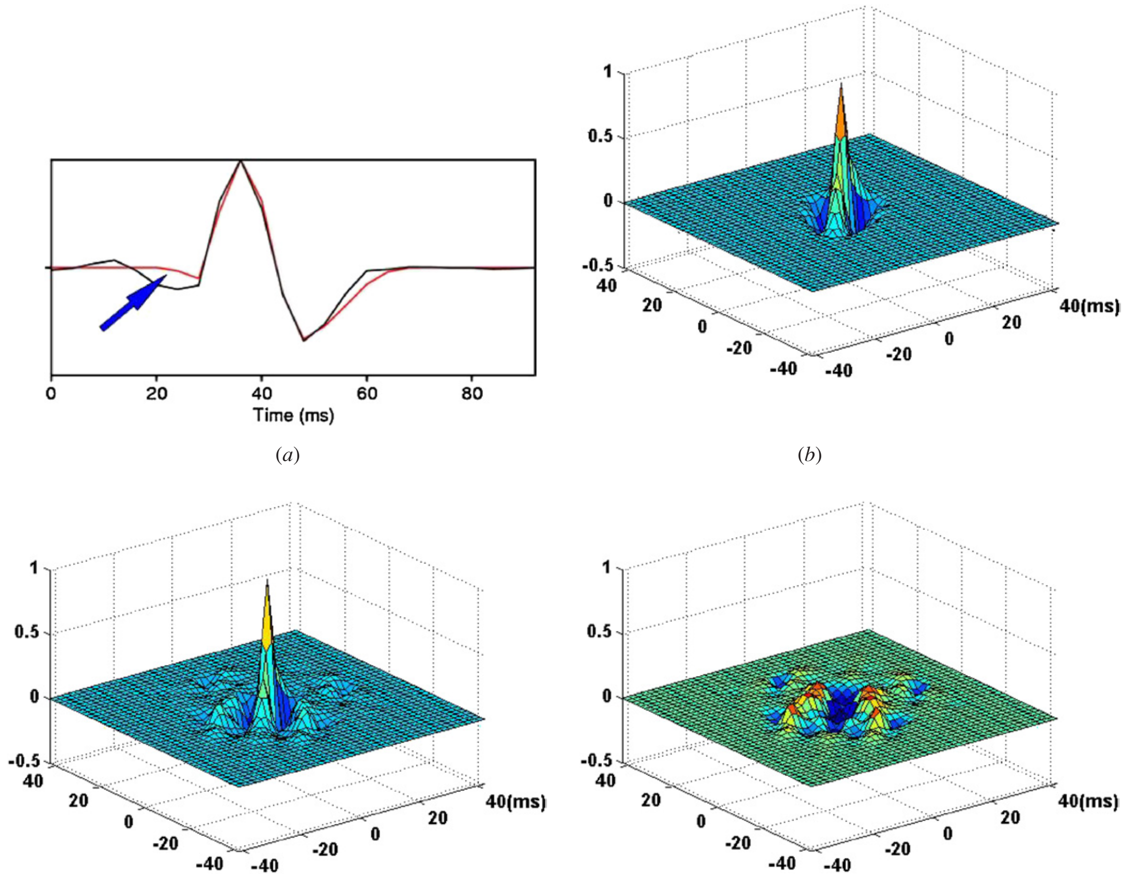

(a) (b) (c) (d)

Figure 6. (*a*) Replot of figure 5(*a*) with the true wavelet (red/grey curve) and the linear inversion result (black curve); the arrow indicates the quench. (*b*) One slice of true wavelet FOM. (*c*) One slice of the estimated wavelet FOM by windowing the seismic trace's fourth-order cumulant. (*d*) The difference between (*b*) and (*c*).

the wavelet estimation is so sensitive to the q value, and thus the NC method is not stable in practice.

4. Wavelet estimation by iterative linear inversion

In this paper, we estimate the wavelet using an iterative linear inversion method to solve a fourth-order moment matching problem.

For wavelet estimation, the MTM and NC methods make use of only single high-order-statistics slices, and both are not stable. To overcome these problems, one may use an inversion method (Lazear 1993, Velis and Ulrych 1996) that minimizes the error in a least-square sense between the calculated fourth-order moment of the wavelet to be estimated and the windowed fourth-order cumulant of the seismic trace,

$$J(w) = \sum_{\tau_1=-q}^{q} \sum_{\tau_2=-q}^{q} \sum_{\tau_3=-q}^{q} \left[\tilde{m}_4^w(\tau_1, \tau_2, \tau_3) - m_4^w(\tau_1, \tau_2, \tau_3)\right]^2, \tag{25}$$

where q is the assumed length of the wavelet to be estimated and $\tilde{m}_4^w(\tau_1, \tau_2, \tau_3)$ is the windowed fourth-order cumulant of the seismic trace (equation (10)). The objective function $J(w)$ is a highly nonlinear multidimensional cost function because it involved high-order covariance computation.

Velis and Ulrych (1996) used a SA technique to solve the optimization problem in equation (25). However, the SA algorithm involves a trade-off between convergence to a global minimum and algorithm speed. Therefore, to speed up the computation, we adopt an iterative linear inversion method in this paper. We formulate this nonlinear minimization problem (25) in a matrix-vector form as

$$\mathbf{F}\Delta\mathbf{w} = \Delta\mathbf{e}, \tag{26}$$

where $\mathbf{F}$ is a matrix of the Fréchet derivatives of the moment function at lag j with respect to the current wavelet vector $w(i)$:

$$\mathbf{F}(j, i) = \partial m_4^w(j)/\partial w(i), \tag{27}$$

and $\Delta\mathbf{e}$ is the residual vector:

$$\Delta\mathbf{e}(j) = \tilde{m}_4^w(j) - m_4^w(j). \tag{28}$$

Then, we solve the model update vector by

$$\Delta\mathbf{w} = (\mathbf{F}^T\mathbf{F} + \mu\mathbf{I})^{-1}\mathbf{F}^T\Delta\mathbf{e}, \tag{29}$$

where μ is the so-called stabilized factor. We set it proportional to the maximum of the diagonal value of $\mathbf{F}^T\mathbf{F}$. Finally, we

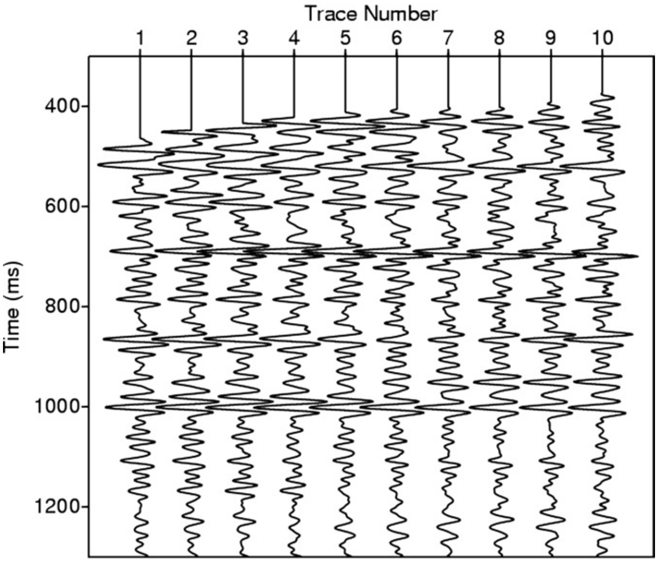

Figure 7. Real seismic traces.

update the wavelet by

$$\mathbf{w}^{(n+1)} = \mathbf{w}^{(n)} + \Delta \mathbf{w}, \tag{30}$$

where n is the iteration number.

Figure 5 shows the test results on the synthetic wavelet. Each of the four cases uses different initial estimates generated by using (*a*) the third-order MTM, (*b*) the fourth-order MTM, (*c*) the third-order NC and (*d*) the fourth-order NC methods, respectively. These initial estimates are plotted as dotted curves, and the linear inversion results are plotted as solid black curves. Each inversion result is also compared to the true wavelet (red/grey curve). The phase spectra of estimated wavelets (black curve) are also compared to the phase spectrum of the true wavelet (in red/grey). After the iterative inversion, phase spectra are better matched to the phase spectrum of the true wavelet.

From all the subplots of figure 5, we can see that there are quenches in the front part of the estimated wavelet where there is relatively greater difference compared with other parts. Figure 6(*a*) takes figure 5(*a*), for example, replotting the true synthetic wavelet in red (grey) and the linear inversion result in black with an arrow indicating the quench. Figure 6(*b*) is the fourth-order moment slice of the true wavelet, and figure 6(*c*) is a slice of the estimated wavelet fourth-order moment by windowing the fourth-order cumulant of the seismic trace. Figure 6(*d*) highlights the difference between figures 6(*b*) and (*c*). This difference is the cause of the quench shown in figure 6(*a*). Further investigation is needed to make the windowed fourth-order cumulant (an approximate fourth-order moment) close to the fourth-order moment of the wavelet.

Figure 7 is a portion of real seismic data used for our mixed-phase wavelet estimation. For real data application, both the MTM method and the NC method are not stable enough to guarantee every trace use, as they make use of only single high-order-statistics slices. The accuracy of the linear inversion method can be guaranteed if a good initial model is supplied, and is suitable for wavelet estimation for a large number of traces. The results of either the MTM or NC method can serve as the initial model for the linear solution of the moment matching method; thus we can get a good estimation for a whole seismic profile.

Figure 8 shows the linear inversion results corresponding to two different initial models. In (*a*) and (*b*), the initial models are generated using the MTM and NC methods, respectively. For each of these two cases, there are three panels: the left panel is the initial estimate, the middle panel shows the linear inversion result of the ten traces in figure 7 and the right panel is the optimal result, selected from the ten wavelets in the middle panel. This optimal wavelet is the wavelet that it is most similar to the other nine trace wavelets. We calculate the correlation functions of any single wavelet with the other nine wavelets, and sum up the correlation coefficients. The optimal wavelet is the one that has the largest summed-up correlation coefficients.

Figure 9 shows a comparison of the fourth-order moment slice between the initial model and the final optimal wavelet.

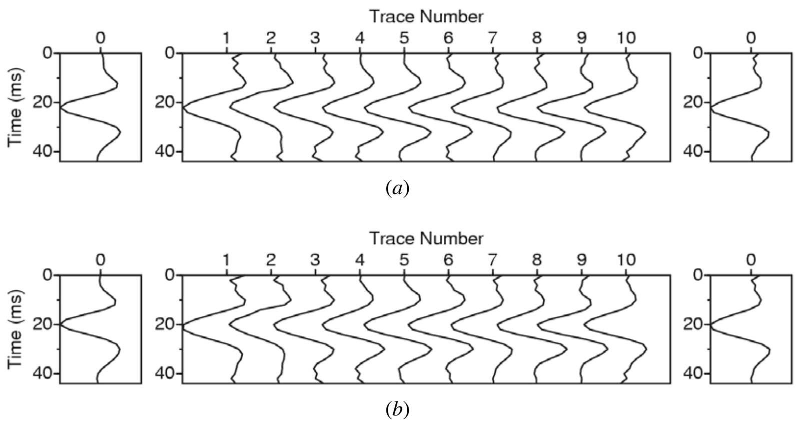

Figure 8. Wavelet estimation of real seismic data using iterative linear inversion. (*a*) and (*b*) are two cases with different initial wavelets, generated using the MTM and NC methods, respectively. For each case, the middle panel is the result of the linear inversion method for the ten traces in figure 7, and the right panel is the final result, an optimal wavelet selected from the ten wavelets in the middle panel.

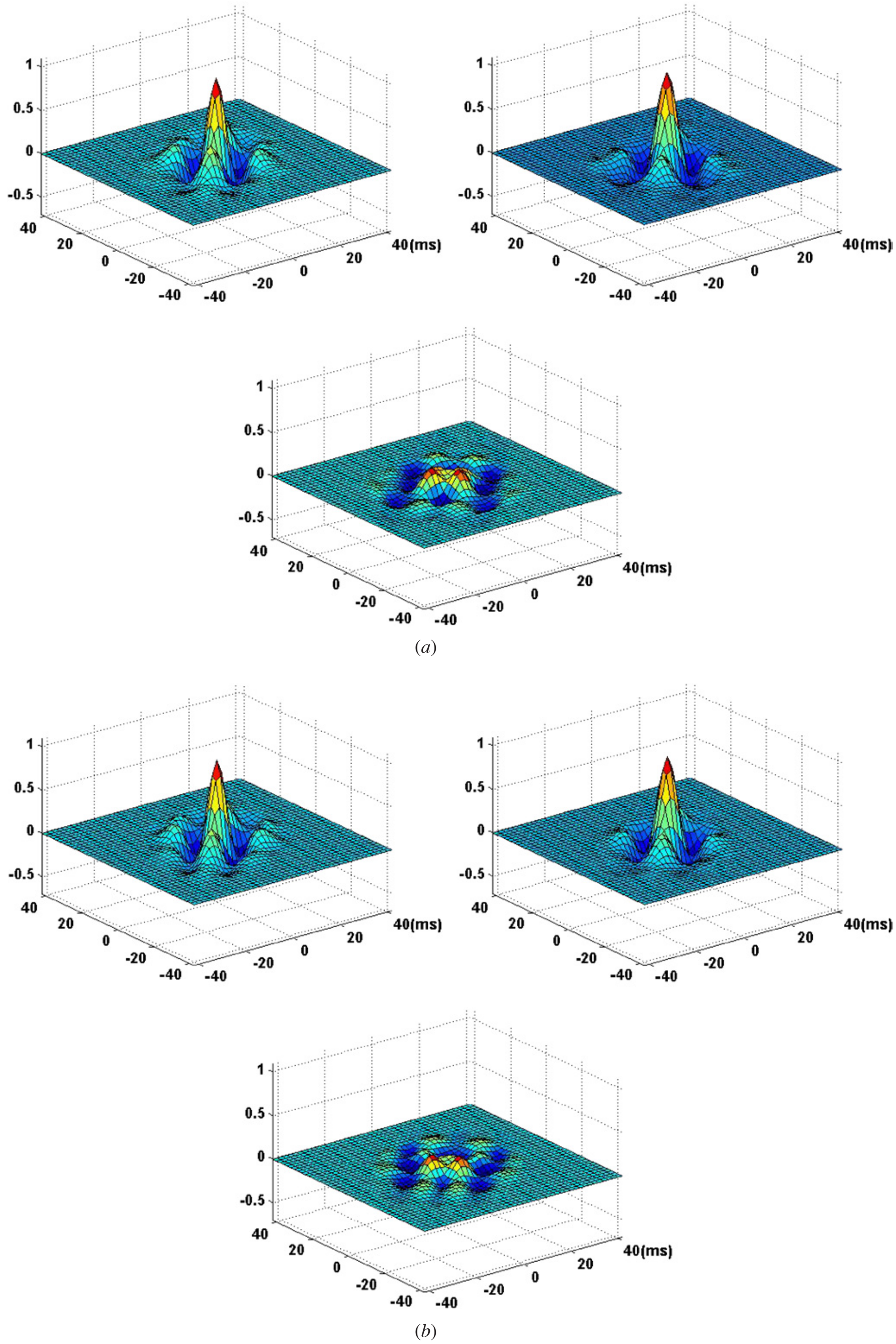

Figure 9. A comparison of the fourth-order moment slices between the initial models and the iterative inversion results. (*a*) and (*b*) correspond to the two cases respectively in figure 8. For each case, we show the FOM slice of the initial model, the FOM slice of the final wavelet and the difference between these two FOM slices.

Figures 9(*a*) and (*b*) correspond to the two cases in figure 8. For each case, we also display the difference between the two fourth-order moment slices. This difference slice visualizes the update of 'data misfit' made by the iterative linear inversion.

5. Conclusions

For mixed-phase wavelet estimation, the MTM and NC methods make use of only single high-order-statistics slices and both are not stable. As for the iterative linear inversion method, it uses the whole fourth-order moment in matching which is reliable and accurate, but needs a good and reliable initial estimate, due to the non-uniqueness of the inversion solution. Therefore, we adopt a hybrid strategy that uses the MTM or NC method to generate an initial wavelet estimate for the iterative linear inversion method for wavelet estimation. This iterative linear inversion method can be applied to multi-channel real seismic data for mixed-phase wavelet estimation. The real data test has shown that all inversion with different initial estimates that are generated from MTM and NC methods converge to the same result within allowable accuracy. However, further investigation is needed to make the windowed fourth-order cumulant of the seismic trace close to the fourth-order moment of the wavelet.

Acknowledgment

We are grateful to the sponsors of the Centre for Reservoir Geophysics, Imperial College London.

Appendix. The maximum time-delayed slice of the moment

The maximum time-delayed slice of the moment can be used to approximate the reflectivity series. For an original derivation, readers may refer to Lu (2005). We summarize it here for the sake of completeness of this review paper.

Assume that the reflectivity $r(t)$ is sparse and can be written as

$$r(t) = \sum_{i=1}^{N} a_i \delta(t - d_i), \tag{A.1}$$

where N is the number of reflectors (non-zero point in the reflectivity function), a_i and d_i are the amplitude and location of the ith reflector, respectively, and $\delta(t)$ is the unit Kronecker delta function. Without loss of generality, we assume $d_j > d_i$ if $j > i$. The maximum time delay of the reflectivity $r(t)$ is defined by

$$D_{\max} = d_N - d_1. \tag{A.2}$$

Substituting equation (A.1) into (1), we obtain

$$m_3^r(\tau_1, \tau_2) = \sum_t \left\{ \sum_{i=1}^{N} [a_i \delta(t - d_i)] \sum_{j=1}^{N} [a_j \delta(t + \tau_1 - d_j)] \times \sum_{k=1}^{N} [a_k \delta(t + \tau_2 - d_k)] \right\} = \sum_{i=1}^{N} \sum_{j=1}^{N} \sum_{k=1}^{N} \times \left\{ a_i a_j a_k \sum_t [\delta(t - d_i) \delta(t + \tau_1 - d_j) \delta(t + \tau_2 - d_k)] \right\}. \tag{A.3}$$

Fixing $\tau_2 = D_{\max}$, we obtain the maximum time-delay slice of the reflectivity third-order moment,

$$m_3^r(\tau_1, D_{\max}) = \sum_{i=1}^{N} \sum_{j=1}^{N} \sum_{k=1}^{N} \left\{ a_i a_j a_k \sum_t [\delta(t - d_i) \times \delta(t + \tau_1 - d_j) \delta(t + D_{\max} - d_k)] \right\}. \tag{A.4}$$

The maximum time-delay slice has non-zero samples only when

$$t = d_i, \qquad i = 1, N, \tag{A.5}$$

$$\tau_1 = d_j - t, \qquad j = 1, N, \tag{A.6}$$

$$d_N - d_1 = d_k - t, \qquad k = 1, N. \tag{A.7}$$

To satisfy (A.5) and (A.7), it is easy to see that i must be equal to 1 and k must be equal to N. Therefore, equation (A.4) can be rewritten as

$$m_3^r(\tau_1, D_{\max}) = a_1 a_N \sum_{j=1}^{N} a_j \delta(\tau_1 - d_j + d_1). \tag{A.8}$$

Comparing with equation (A.1), the maximum time-delay slice (A.8) is a scaled and time-shifted version of the reflectivity. Let

$$\tilde{r}(t) = m_3^r(t, D_{\max}); \tag{A.9}$$

the reflectivity series in the frequency domain can be obtained by

$$r(\omega) = \tilde{r}(\omega)\, \mathrm{e}^{-\mathrm{i}\omega d_1} / (a_1 a_N). \tag{A.10}$$

That is, the maximum time-delayed slice of the third-order moment may be used to estimate the reflectivity series. Note that the denominator in equation (A.10) is not responsible for the phase spectrum estimation.

References

Giannakis G B 1987 Cumulants: a powerful tool in signal processing *Proc. IEEE* **75** 1333–4

Giannakis G B and Delopoulos A 1995 Cumulant-based automation estimates of non-Gaussian linear process *Signal Process.* **47** 1–17

Lazear G L 1993 Mixed-phase wavelet estimation using fourth-order cumulants *Geophysics* **58** 1042–51

Lu W 2005 Non-minimum-phase wavelet estimation using second- and third-order moments *Geophys. Prospect.* **53** 149–58

Lu W and Zhang Y 2006 Reply to Comment on ‘Non-minimum-phase wavelet estimation using second- and third-order moments’ by W Lu *Geophys. Prospect.* **54** 489–90

Lu W, Zhang Y, Zhang S and Xiao H 2007 Blind wavelet estimation using a zero-lag slice of the fourth-order statistics *J. Geophys. Eng.* **4** 24–30

Mendel J M 1991 Tutorial on higher-order statistics (spectra) in signal processing and system theory: theoretical results and some applications *Proc. IEEE* **79** 278–305

Sacchi M D and Ulrych T J 2000 Non-minimum-phase wavelet estimation using higher order statistics *Leading Edge* **19** 81–3

Velis D R and Sacchi M D 2006 Comment on ‘Non-minimum-phase wavelet estimation using second- and third-order moments’ by W Lu *Geophys. Prospect.* **54** 487–8

Velis D R and Ulrych T J 1996 Simulated annealing wavelet estimation via fourth-order cumulant matching *Geophysics* **61** 1939–48